Available online at www.sciencedirect.com
SCIENCE DIRECT
Geochimica et Cosmochimica Acta 70 (2006) 3533–3548
Geochimica
www.elsevier.com/locate/gca

Groundwater N speciation and redox control of organic N mineralization by O_2 reduction to H_2O_2

John W. Washington [a,*], Robert C. Thomas [a], Dinku M. Endale [b], Katherine L. Schroer [c], Lidia P. Samarkina [d,a]

[a] USEPA, National Exposure Research Laboratory, 960 College Station Road, Athens, GA 30605, USA
[b] USDA-ARS, J. Phil Campbell, Sr., Natural Resource Conservation Center, 1420 Experiment Station Road, Watkinsville, GA 30677, USA
[c] University of Georgia, Department of Geology, Geography-Geology Building, Athens, GA 30602, USA
[d] Senior Service America, Inc., USA

Received 26 June 2005; accepted in revised form 12 April 2006

Abstract

Excess N from agriculture induces eutrophication in major river systems and hypoxia in coastal waters throughout the world. Much of this N is from headwaters far up the watersheds. In turn, much of the N in these headwaters is from ground-water discharge. Consequently, the concentrations and forms of N in groundwater are important factors affecting major aquatic ecosystems; despite this, few data exist for several species of N in groundwater and controls on speciation are ill-defined. Herein, we report N speciation for a spring and well that were selected to reflect agricultural impacts, and a spring and well that show little to no agricultural-N impact. Samples were characterized for NO_3^-, NO_2^-, N_2O, NH_4^+, urea, particulate organic N(N^p_{org}), and dissolved organic N(N^d_{org}). These analytes were monitored in the agricultural spring for up to two years along with other analytes that we reported upon previously. For all samples, when oxidized N was present, the dominant species was NO_3^- (88–98% of total fixed N pool) followed by N^d_{org} (<4–12%) and only trace fractions of the other N analytes. In the non-agriculturally impacted well sample, which had no quantifiable NO_3^- or dissolved O_2, N^d_{org} comprised the dominant fraction (68%) followed by NH_4^+ (32%), with only a trace balance comprised of other N analytes. Water drawn from the well, spring and a wetland situated in the agricultural watershed also were analyzed for dissolved N_2 and found to have a fugacity in excess of that of the atmosphere. H_2O_2 was analyzed in the agricultural spring to evaluate the O_2/H_2O_2 redox potential and compare it to other calculated potentials. The potential of the O_2/H_2O_2 couple was close in value to the NO_3^-/NO_2^- couple suggesting the important role of H_2O_2 as an O_2-reduction intermediate product and that O_2 and NO_3^- are reduced concomitantly. The O_2/H_2O_2 and NO_3^-/NO_2^- couples also were close in value to a cluster of other inorganic N and Fe couples indicating near partial equilibrium among these species. Urea mineralization to NO_2^- was found to approach equilibrium with the reduction of O_2 to H_2O_2. By modeling N^d_{org} as amide functional groups, as justified by recent analytical work, similar thermodynamic calculations support that N^d_{org} mineralization to NO_2^- proceeds nearly to equilibrium with the reduction of O_2 to H_2O_2 as well. This near equilibration of redox couples for urea- and N^d_{org}-oxidation with O_2-reduction places these two couples within the oxidized redox cluster that is shared among several other couples we have reported previously. In the monitored agricultural spring, $[NO_3^-]$ was lower in the summer than at other times, whereas $[N_2O]$ was higher in the summer than at other times, perhaps reflecting a seasonal variation in the degree of denitrification reaction progress. No other N analytes were observed to vary seasonally in our study. In the well having no agricultural-N impact, $C_{org}/N_{org} = 5.5$, close to the typical value for natural aqueous systems of about 6.6. In the agricultural watershed C_{org}/N_{org} varied widely, from $\sim$1.2 to $\gtrsim 9$.

1. Introduction

Each spring, excess nitrogen flowing from the Mississippi River fuels the formation of a vast hypoxic zone in the Gulf

* Corresponding author. Fax: +1 706 355 8202.
E-mail address: washington.john@epa.gov (J.W. Washington),

0016-7037/$ - see front matter © 2006 Elsevier Inc. All rights reserved.
doi:10.1016/j.gca.2006.04.006

of Mexico. When the nitrogen-rich Mississippi waters enter the naturally nitrogen-limited Gulf, algae, and other micro-organisms bloom in huge numbers, die, settle to the bottom, decay, and, in so doing, deplete the bottom waters of oxygen. Seasonally expanding to as large as 20,000 km^2 (Goolsby, 2000), this hypoxia kills poorly mobile, bottom-dwelling organisms, thereby disrupting the fishing industry along the Louisiana and Texas coasts.

The Gulf is not suffering such impacts alone; commercially and environmentally important coastal waters world-wide—the Chesapeake Bay, the Baltic Sea, the northern Adriatic Sea, the Gulf of Thailand, and the Yellow Sea—all are experiencing similar problems (UNEP, 2003). And the Mississippi River is not alone in transporting N-enriched waters either; N over-enrichment has been implicated as causing eutrophication in 60% of US coastal rivers and bays (Showstack, 2000).

Problems arising from nutrient-fueled algal blooms are not limited to hypoxia. The toxic red tides off the Gulf coasts and the *Pfiesteria piscicida* in mid-Atlantic coastal rivers both may be promoted by nutrient over-enrichment (Showstack, 2000).

While these conspicuous problems take place in the large waterbodies off the coasts and higher-order rivers, most of the nutrients that induce these problems flow with source waters from far up the watersheds (Goolsby, 2000), especially headwater and other small streams (Peterson et al., 2001). In turn, much of the water these small streams receive is supplied by groundwater discharge, typically on the order of 55% of the total flow (Winter et al., 1998). As a consequence, the concentrations and forms of N in groundwater are important factors affecting the aquatic ecosystems along our coasts. Despite this influential role, for several N species, few groundwater data have been reported and some N transformation processes in the subsurface are ill-defined as well.

The most common species of N in contaminated groundwater is NO_3^- and multiple e^- donors have been identified or implicated in the reduction of NO_3^- in groundwater settings (Korom, 1992). In a sandy glacial aquifer contaminated by treated waste-water, Desimone and Howes (1996) found denitrification to be controlled by the most conventionally cited e^- donor for denitrification, i.e., C_{org}. On the other hand, mineral e^- donors commonly appear to be important as well; Korom et al. (2005) determined that S^{-1} from FeS_2 was the dominant e^- donor for NO_3^- reduction in a glacial outwash aquifer and Bohlke and Denver (1995) argued that Fe^{2+} in glauconite served as the predominant e^- donor for NO_3^- reduction in a coastal aquifer.

NO_3^- reduction in the subsurface appears to exhibit a variety of activity patterns, both spatially and in terms of relative rates between denitrification steps. Ueda et al. (2003) reported that the highest potential denitrification activity overlapped aquifer areas where they observed highest [NO_3^-]. Alternatively, Tesoriero et al. (2000) observed most denitrification to take place in a 'redoxicline' wherein the oxidation state of multiple species changed dramatically. Differently still, Smith et al. (2004) reported that denitrification appeared to take place preferentially in discrete flow paths relative to other locations. Regarding relative rates among the multiple denitrification steps, Smith et al. (2004) found that $NO_3^- \rightarrow NO_2^-$ proceeded more quickly than subsequent denitrification steps.

McGuire et al. (2002) showed that most denitrification in groundwater takes place at, or in association with, solid surfaces. This surface association for denitrification might play a role in the observation that nitrate reduction is much less effectual in fields/aquifers that have been tiled to enhance drainage; David et al. (1997) reported that roughly 50% of N applied to tiled agricultural fields made its way to local rivers. However, some of this effect appears to be a consequence of simple short circuiting as well because most of this N loss from tiled fields occurred subsequent to a few high precipitation events (David et al., 1997).

N_2O in groundwater has been reported as commonly occurring in excess of that for water in equilibrium with the atmosphere. Most of this excess N_2O has been interpreted as being generated by nitrification in the vadose zone (Muhlherr and Hiscock, 1998; Ueda et al., 1991). However, N_2O also apparently can be generated by denitrification in the saturated zone as well (Muhlherr and Hiscock, 1998).

Information on the occurrence of, and factors affecting the fate of, organic N (N_{org}) in groundwater is more sparse than for most of the inorganic N species. This data gap for N_{org} in groundwater is significant because, in many nitrogen-degraded rivers (Maybeck, 1982) and streams (Willett et al., 2004), N_{org} is the second-most concentrated N species after NO_3^-, typically comprising about 40% of the total dissolved-N pool (Maybeck, 1982; Willett et al., 2004).

The N_{org} fraction of most environments predominantly is present in humic and fulvic materials (Aiken et al., 1985). Large fractions of this N_{org} have been observed to be persistent in the environment, commonly 30–50% in terrestrial settings (Schulten and Schnitzer, 1997) and the majority in the oceans (McCarthy et al., 1997). Historically, this persistent N_{org} fraction was thought to be comprised largely of stabilized complex macromolecular heterocyclic compounds (Knicker and Ludemann, 1995). Yet analytical work during the last decade shows that the majority of terrestrial (Knicker and Ludemann, 1995), riverine (Vairavamurthy and Wang, 2002), and marine (McCarthy et al., 1997) N_{org} is present as amide functional groups, probably as proteins. Proteinaceous materials generally are labile (Vairavamurthy and Wang, 2002) and this incongruity with the observation of persistent N_{org} fractions has spurred several theories regarding the cause of this persistence, mostly focusing on molecular changes that might impart a refractory nature to these otherwise-labile moieties (Vairavamurthy and Wang, 2002; Zang et al., 2000). In N-rich settings, mineralization of N_{org} commonly is executed by microbes to garner metabolic energy, that is, as exergonic reactions. Because of this, and because of the open

question regarding the cause of the apparent persistence of labile N_{org} moieties, a reasonable question is whether some N_{org} might persist because it nearly has equilibrated with system oxidants rather than because it is refractory.

In this paper, we report N-speciation data for groundwater in both N-impacted settings and settings showing little to no excess N; the number of species we report is rare for groundwater and includes particulate organic N (N^p_{org}), dissolved organic N (N^d_{org}), urea N ($NH_3(CO)_{0.5}$), NO_3^-, NO_2^-, N_2O, NH_4^+, and dissolved N_2. We analyze H_2O_2 to compare the potential of the O_2/H_2O_2 redox couple to other N-couple potentials. We examine the hypothesis that some N_{org} might persist because it approaches partial equilibrium with its surroundings rather than because of any real refractory nature and we compare the C_{org}/N_{org} status of these groundwaters to other aquatic systems.

2. N speciation and transformations

Nitrogen commonly occurs in seven redox states and transformation between these states typically is mediated biologically, chiefly microbially below the root zone (Fig. 1). The dominant atmospheric N species, N_2, is triply bonded between the atoms, N≡N, making the molecule remarkably stable. Consequently, biological N fixation, where N_2 is converted to NH_3 and then to N^p_{org}, is an energetically costly process carried out only by a few prokaryotes and symbiotic microbes (Brock et al., 1994).

Upon cell death, N^p_{org} is subject to assimilative and dissimilative ammonification. In dissimilative ammonification, organic matter is used as a C source with an attendant release of NH_4^+ (Zubay, 1993). Although there is no change in N-oxidation state during dissimilative ammonification, N presumably can play a role in the effi-

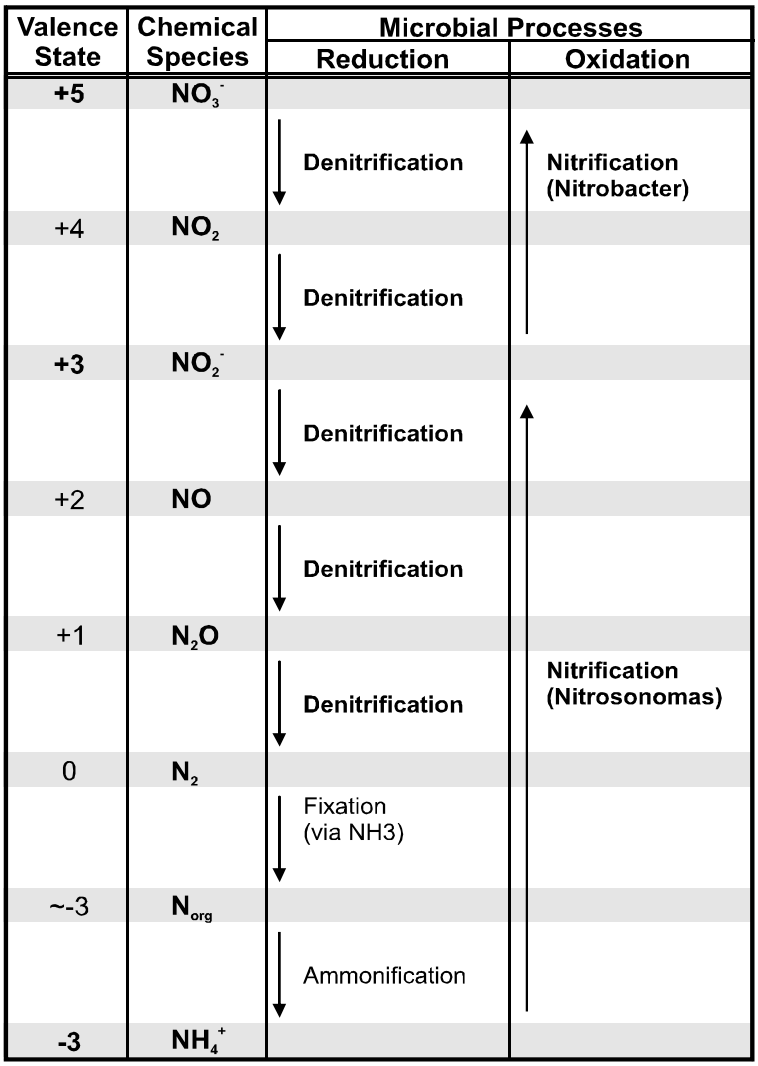

Fig. 1. N transformations—emboldened species are the dominant forms for biological assimilation and emboldened processes can be exergonic. Together, ammonification and nitrification often are coined mineralization. Nitrogen species, excluding N_2, often are grouped under the heading 'fixed N' or 'reactive N,' in reference to their common trait of having undergone fixation and being readily available for one or more biological transformations.

ciency of catabolism in the protonation of the organic –NH_2 group to form NH_4^+.

Under oxidizing conditions, NH_4^+ is oxidized, or nitrified, as an energy source by chemotrophic bacteria, commonly in two steps, $NH_4^+ \rightarrow NO_2^-$ and $NO_2^- \rightarrow NO_3^-$. The genus *Nitrosomonas* mediates the first nitrification step in both soil and aqueous settings, *Nitrosococcus* mediates step one in aqueous settings only, and *Nitrosospira*, *Nitrosolobus*, and *Nitrosovibrio* mediate step one in soil only (Brock et al., 1994). The genus *Nitrobacter* mediates the second nitrification step in both soil and aqueous settings, while *Nitrospina*, *Nitrococcus*, and *Nitrospira* mediate step two in marine settings only (Brock et al., 1994). In oxic settings, ammonification and nitrification often are closely coupled, and together these processes commonly are coined mineralization.

In turn, NO_3^- is subject to both assimilative and dissimilative reduction. In dissimilative reduction, or denitrification, oxidized N species act as respiratory electron acceptors to produce any of five oxidation states between NO_2 and N_2 (Fig. 1). For denitrification reactions, organic carbon (C_{org}) is widely recognized as the primary electron source; however, chemotrophic microbial reduction of NO_3^- also can proceed using Fe^{2+} (Straub et al., 1996), and HS^- and S^- (Appelo and Postma, 1996; Korom et al., 2005) as sole electron donors.

3. Materials and methods

Waters were sampled from four subsurface-flow-system sources located in the Southern Piedmont Physiographic Province, Oconee County in northeastern Georgia. At all sample locations, bedrock is gneiss (Railsback et al., 1996) and the lithologic unit is designated as Athens Gneiss. Based on well cuttings and outcrops in the study area, Athens Gneiss predominantly is granodioritic gneiss locally. Soil series are comprised mostly of Cecil series and Pacolet series, both classified clayey, kaolinitic, thermic Typic Kanhapludult.

Three of the sample locations are on United States Department of Agriculture (USDA) Agricultural Research Service property, the J. Phil Campbell Senior Natural Resource Conservation Center (Amirtharajah et al., 2002), about 10 km south of the United States Environmental Protection Agency (USEPA) lab in Athens, GA where the analyses were performed. Well NU18 and Spring SpW2 are about 60 m apart. They combine to represent mid-flowpath and discharge locations, respectively, of the USDA Watershed 2, an area of about 10 ha. This watershed, encompassed entirely within USDA property, is comprised mainly of pasture through which about 100 cow-calf pairs are rotated roughly one week in six. In addition to nutrients and C_{org} from cattle waste, Watershed 2 also is fertilized at a rate of about 78 kg N/(ha-yr). The uppermost aquifer flow is through the saprolite which ranges from about <8 to >21 m depth. Spring SpW2 was sampled for most analytes about two dozen times over about two years. Well NU18 extends to the top of bedrock, 11 m, and is screened over the bottom 3 m. Application of the Jacob straight-line drawdown method (Driscoll, 1989) to pumping test data from Well NU18 led to a hydraulic conductivity of about 2×10^{-5} to 3×10^{-5} cm/s. The hydraulic gradient between NU18 and SpW2 ranges from about 0.02 to 0.04.

Spring NWSp is about one km NNW of Spring SpW2, set in a wooded area of the USDA property that is in a separate watershed from Well NU18 and Spring SpW2. It is similar to Spring SpW2 except that it issues from an area used less intensively for agriculture and in which no cattle are grazed.

The Hillcrest Well, a public water-supply well drilled into granodioritic gneiss to a depth of about 177 m, is located about 3.5 km west of USDA Watershed 2 in a separate watershed from the other three sampling points. It was sampled from a tap on the well head during its normal, continuous-production pumping of about 340 L/min.

The well (Well NU18) and the spring (SpW2) draining the beef-cattle pasture were chosen to represent a system that clearly has been impacted by agriculture while the deep well into bedrock (Hillcrest Well) and the wooded spring (NWSp) were chosen to represent systems located in similar geologic settings and having little or no agricultural impact.

For springs, an effort was made to transfer the water from as near to the source of issuance as possible by syphoning or peristaltic pumping into a container where flow was from the bottom upwards to spill over the container lip continuously so that samples could be collected having virtually no contact with air. For wells, samples were collected only after stable readings were achieved for pH (Orion Model 250A+), specific conductance (YSI Model 30), dissolved O_2 (YSI Model 55) and temperature (using thermocouples on the pH, specific conductance and O_2 probes); these samples also were collected from an upwelling, overflowing container. YSI reports the detection limit for the Model 55 dissolved O_2 probe to be 9 μM, a conservatively high value that varies between meters and with wear on the sensor membrane.

Collected samples were subjected to numerous analyses for redox-sensitive solutes. In an earlier paper (Washington et al., 2004) we reported the analytical results for specific conductance, pH, temperature, $[O_2]$, $[H_2]$, alkalinity, $[H_2CO_3]$, [CO], $[CH_4]$, $[C_{org}]$, $[NO_3^-]$, $[NO_2^-]$, $[N_2O]$, $[NH_4^+]$, $[SO_4^=]$, $[H_2S]$, [Fe(II)], [Fe(III)], and $[Cl^-]$.

The new analyses we report herein for N^p_{org}, N^d_{org}, and urea for the period 2001–2003 were performed on samples that had been composited from three samples from this earlier work (Washington et al., 2004) and preserved by freezing.

3.1. Particulate and dissolved total N

Total N was analyzed by oxidation of all fixed N in a sample, followed by analysis for NO_3^-. Common modes

of N oxidation include persulfate, ultra-violet, and high-temperature oxidation. In a comparison of oxidation methods for N in water samples, Bronk et al. (2000) showed that persulfate oxidation consistently had the highest percentage recovery of the three methods.

Our persulfate oxidizing solution followed the recipe of Eaton et al. (1995) and consisted of 0.2 M $K_2S_2O_8$ (Fisher ACS Grade), 0.5 M $B(OH)_3$ (Fisher ACS Grade) and 0.1 M NaOH (Fisher 50% w/w ACS Grade). In each sample run, 10 mL of nanopure H_2O (blank), glycine standard ($C_2H_5NO_2$; from LabChem 20% w/v Reagent Grade) or sample were pipetted into culture tubes and labeled. One mL of oxidizing solution was added to each culture tube, the tubes were capped tightly, vortexed and autoclaved at 121 °C for 40 min. Each sample was digested in two tubes, with unfiltered sample in 1 and 0.2-μm, Teflon-filtered sample in the other; these samples were designated, respectively, as total N (N_t) and dissolved total N (N_t^d). After autoclaving, the originally unfiltered N_t samples were filtered to prepare them for analysis.

Prior to 2005, samples were analyzed using a Dionex DX-500 ion chromatograph with an ASRS Ultra electrolytical suppressor, Dionex Ionpac standard-bore AS-15 guard and separating columns, and an anion trapping column to suppress carbonate following the method of Washington et al. (2004). Reagent blanks had small, but quantifiable, concentrations, typically about 2% of sample values. Consequently, reagent blank concentrations were subtracted from the analytical concentrations of N_t and N_t^d, and the results were multiplied by a 1.1-dilution factor to correct for the addition of the oxidant.

Starting with our blank- and dilution-corrected values, particulate total N (N_t^p) is defined as:

$$[N_t^p] = [N_t] - [N_t^d]. \quad (1)$$

Our limit of detection (LOD) for N_t^p was 28 μM. We detected N_t^d in all our samples well in excess of its LOD of 14 μM.

3.2. Particulate and dissolved organic N

Dissolved organic N (N^d_{org}) is defined as:

$$[N^d_{org}] = [N_t^d] - [NO_3^-] - [NO_2^-] - [NH_4^+]. \quad (2)$$

Particulate organic N (N^p_{org}) is defined as:

$$[N^p_{org}] = [N_t] - [NO_3^-] - [NO_2^-] - [NH_4^+] - [N^d_{org}]. \quad (3)$$

We exclude N_2O from N_{org} calculations because the samples were exposed to the atmosphere during sample preparation and we assume most N_2O volatilized before sample digestion. Operationally, $[N^p_{org}]$ is equivalent to $[N_t^p]$. Since NO_3^- comprised the largest fraction that was subtracted from N_t and $[N_t^d]$ to solve for N_{org} in most of our samples, small errors in $[NO_3^-]$ were found to result in large errors in our N_{org} values. To minimize such errors, undigested aliquots were analyzed for $[NO_3^-]$ on the same day as the digested samples representing $[N_t]$ and $[N_t^d]$. We checked our recovery of N^d_{org} using glycine as the standard organic-N source, routinely running glycine at several concentrations for every analysis run; for $[N^d_{org}] = 36$–71 μM, the general range of our samples, our recovery averaged 87–94%, respectively, consistent with the recoveries reported by Bronk et al. (2000). In samples having detectable NO_3^-, our LOD for N^d_{org} was 14 μM. When NO_3^- was not detectable, no uncertainty was imparted to our calculation of $[N^d_{org}]$ by NO_3^- and, for these samples, our LOD was lower, 7 μM.

3.3. Urea N

Urea was measured by adding urease and a pH buffer to water samples and standards, and allowing reaction for 30 min to cleave the amines from the carbonyl. Then samples and standards were prepared for NH_3 analysis by the phenate method (Clesceri et al., 1998), with the modification of allowing reaction and settling overnight to minimize turbidity.

The pH buffer was 0.04 M trisodium phosphate dodecahydrate ($Na_3PO_4{\cdot}12H_2O$; EM Science ACS Grade), 0.036 M sodium dihydrogen phosphate monohydrate ($NaH_2PO_4{\cdot}H_2O$; EM Science ACS Grade) and 0.04 M EDTA disodium dihydrate (Baker Reagent Grade). The urease suspension was prepared with 2 g lyophilized urease (EM Science specified $\geqslant 5$ U/mg) in 10 mL glycerin (Fisher ACS Grade) and 10 mL water (EM Science ACS grade), and was kept in suspension with a magnetic stir bar. In every sample run, several calibration standards were prepared from the urea reagent and analyzed.

For each filtered sample, standard and blank, 3 mL were pipetted into a 4.5 mL methacrylate disposable cuvette along with 20 μL of the pH buffer. Each cuvette also received one drop of the urease suspension from a Pasteur pipette, the suspension being too viscous to use an autopipette. The cuvettes containing these preparations were allowed to react for 30 min at which time the reagents for phenate analysis of NH_3 were added (Clesceri et al., 1998; Washington et al., 2004). These samples then were allowed to react in the dark overnight, during which time any suspended particles from the urease settled out of the spectrometer's light path. In the morning, post-urease N (N_{pu}) was measured with the spectrometer set to $\lambda = 640$ nm per the phenate method (Clesceri et al., 1998) on a Hach 2010 spectrometer.

The phenate reagents also were added to samples having no urease to measure non-urease-derived $[NH_3]$. The spectrometer was zeroed on pure water having no reagents for all measurements. Urea N was calculated from analytical values by:

$$[NH_3(CO)_{0.5}] = [N_{pu}] - [NH_3]. \quad (4)$$

For this method, the estimated LOD was 0.9 μM N.

3.4. Collection and measurement of dissolved N_2

Dissolved N_2 samples were collected in September 2002 from well NU18, and in June 2005 from well NU18, spring SpW2 and the wetland into which SpW2 issues, about 70-m downgradient of the spring. These samples were collected in gas-sampling jars (Washington et al., 2004) after they had been purged with Grade 5 He (99.999%; BOC Gases). The water samples and headspace were equilibrated, and the headspace analyzed on an Agilent AT 6890 gas chromatograph (GC) with two 2-mL sampling loops in series attached by two ten-port valves that separated flow to: (1) a Hayesep Q column (4 ft × 1/8 in o.d., 80/100 mesh) attached to a 5-ft Hayesep N column (6 ft × 1/8 in o.d., 80/100 mesh) then to a micro electron-capture detector (μECD) using a 95% Ar/5% CH_4 carrier gas; and (2) a Hayesep DB-packed column (30 ft × 1/8 in o.d., 80/100 mesh) leading to a thermal-conductivity detector (TCD) using Grade 5 He. The headspace N_2 was detected on the TCD.

During attempts to generate calibration curves, mixing gas standards for the low [N_2] of our samples proved difficult because of contamination from the high concentration of N_2 in air. We achieved reproducible N_2 peak areas in He headspace from deionized water that had been saturated with atmospheric air by bubbling the air through the water for >1 h. These peak areas were taken to reflect a fugacity (f_{N_2}) of 0.782 atm and N_2 peak areas for Grade 5 He were taken as $f_{N_2} = 0$ to generate a two-point calibration. Original dissolved [N_2] was calculated from headspace [N_2] using a Henry's Law $K_H^{N_2} = 1450$ L-atm/mol (Wilhelm et al., 1977).

3.5. Measurement of H_2O_2

Hydrogen peroxide was analyzed by H_2O_2-oxidative dimerization of (*p*-hydroxyphenyl)acetic acid (POHPAA) followed by fluorescent detection (Herut et al., 1998; Miller and Kester, 1988) with a near-uv lamp, and optical filters for emission, $\lambda_{em} = 320$ nm, and excitation, $\lambda_{ex} = 400$ nm, on a portable Turner 10-AU-005-CE fluorometer. For this method, we reacted 100 μL of fluorometric reagent, consisting of 0.25 mM POHPAA (Aldrich, 98%), 2.1×10^4 purpurgallon U/L peroxidase (Aldrich, stabilized), and 0.25 M tris buffer at pH 8.8 (Sigma), with 5 mL of water for 15 min to dimerize the POHPAA. Fluorescence of the POHPAA dimer is directly proportional to H_2O_2, however fluorescence also occurs as a consequence of other trace species and the fluorometric reagent (Herut et al., 1998; Miller and Kester, 1988). The POHPAA dimer is stable for several hours (Herut et al., 1998; Miller and Kester, 1988) and the fluorescence of the POHPAA-stabilized samples, therefore, can be measured in the laboratory. However, correction for the fluorescent contributions from other trace fluorescing species necessitates measuring of the natural water in the absence of any reagents; natural water is not fluorescently stable (Holm et al., 1987), so we performed our fluorometric measurements in the field. The fluorescent contribution from other species and the fluorometric reagent is quantitated using an H_2O_2-blank value (Blank) that is calculated from: (1) fluorescence of natural water (Nat); (2) water reacted with 50 μL of 8.7×10^7 U/L catalase (Sigma, 2× crystallized) for 5 min (Cat); and (3) the catalase sample with fluorometric reagent added for 15 min (Flr) according to Blank = Nat + (Flr − Cat). The catalase reacts with H_2O_2 but not other trace fluorescing species. As such, subtraction of blank fluorescence from the fluorescence of a water sample reacted with fluorometric reagent solves for fluorescence in the water that is consequent solely of H_2O_2 reacted with POHPAA. However, because of the confounding effects of the trace fluorescing compounds, sample H_2O_2 fluorescence in natural water cannot be related to sample [H_2O_2] by a conventional standard curve. Consequently, sample [H_2O_2] is evaluated by the method of standard additions for which we added 50 μL aliquots of 10^{-6} M H_2O_2 (Solvay Chemicals, cosmetics grade, certified 35.2% assay). The blank fluorescence is subtracted from the fluorescence of the water sample and each standard addition to generate values reflecting fluorescence solely due to H_2O_2, i.e., that naturally occurring in the water sample and that added for the standard additions (Fig. 2). These data plot linearly in fluorescence-added [H_2O_2] space and extrapolation of the line to the [H_2O_2] axis defines the [H_2O_2] in the natural water. Limit of detection for this method, defined as three times the standard deviation of three blank measurements (Herut et al., 1998; Miller and Kester, 1988) was determined to be 1.5 nM.

In performing these analyses, we found that the fluorescence of some samples increased during exposure to light. With regard to this instability, we made these observations: within each sample the rate of fluorescence increase appeared roughly constant for a given condition; the rate of increase was fastest in direct sunlight, slower in indirect

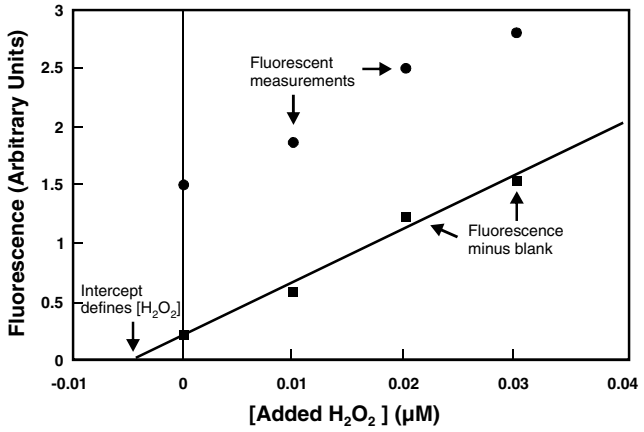

Fig. 2. Solving for [H_2O_2] by method of standard additions. When the blank fluorescence, representing fluorescence due to reagents and trace fluorescent solutes other than H_2O_2, is subtracted from fluorescence readings for the raw sample and standard additions, extrapolation of the linear trend to the intercept defines [H_2O_2].

natural light and slowest to non-existent in artificial light; in all cases, the fluorescence of samples remained stable after the initial 15-min reaction period when they were stored in the dark; and using freshly mixed reagents for each sampling round, we observed no differences in sample stability among reagent batches. We interpreted these observations as probably reflecting photocatalyzed oxidation of organic matter coupled to reduction of O_2 to form H_2O_2.

3.6. Collection and measurement of N_2O, NO_2^-, NH_4^+, C_{org}, and O_2

We originally reported our 2001–2003 data for N_2O, NO_2^-, NH_4^+, C_{org}, and O_2 in Washington et al. (2004); we have resummarized them here (Table 1) for the convenience of the reader. The 2005 data we report for these analytes were generated employing the same techniques described in detail in our earlier work (Washington et al., 2004). In summary, analytical techniques are: N_2O, GC/ECD; NO_2^-, diazotization/spectrometer; NH_4^+, phenate/spectrometer; C_{org}, total-organic-carbon analyzer; and O_2, dissolved-oxygen probe.

3.7. Collection and measurement of other analytes in 2005 sampling rounds

In order to optimize comparison of our 2005 data with our earlier study (Washington et al., 2004), we analyzed all the parameters we included in the earlier study as well. Analytical methods that remained the same for both studies are: H_2, CH_4, and CO_2, GC/TCD; Fe(II) and Fe(III), ferrozine/spectrometer; and HS^-, methylene blue/spectrometer. Details of these analytical efforts are described in our earlier work (Washington et al., 2004).

Anions including NO_3^-, Cl^-, SO_4^{2-}, and HPO_4^{2-} were analyzed on a modular Metrohm-Peak dual-channel ion chromatograph using a 20 μL injection loop, chemical suppressor, and a Metrosep A Supp 5–250 column. Analytical runs of 35 min were performed isocratically at a flow rate of 0.7 mL/min using an anion eluent of 3.2 mM Na_2CO_3 (Baker Reagent Grade) and 0.2 mM $NaHCO_3$ (Baker ACS Grade). Detection limits for all reported analytes were well below that detected in samples.

4. Results

Our 2001–2003 N data are summarized in Table 1. Total fixed dissolved N concentrations, by summing N_t^d and N_2O, varied from 0.01 mM in the deep Hillcrest Well to 0.8 mM in spring SpW2 which drains the beef-cattle pasture. In contrast, particulate N was very small, present at less than the limit of detection in all samples but three from the monitored spring.

Of the four sampling locations, three had quantifiable dissolved O_2 and other oxidized species (Table 1); the Hillcrest Well did not have quantifiable O_2 or NO_3^-. For the three oxidized sample locations, NO_3^- was the dominant N species, present at $\geqslant$0.1 mM in all cases (Table 1) and comprising $\gtrsim$ 90% of N_t^d. The highest observed $[NO_3^-]$, 0.7 mM in spring SpW2, equals the USEPA drinking-water maximum contaminant limit (MCL), but all other samples were less than the MCL. In these three shallower, oxidizing locations, N^d_{org} was the second most-concentrated species at about <14 to 80 μM (Table 1), comprising <2 to 11% of N_t^d (Table 2).

In the deeper, more-reducing Hillcrest well, N was much more dilute than in the shallower, more-oxidizing sample sources. Measured at 9 μM (Table 1), N^d_{org} was the dominant N species in the Hillcrest sample, comprising 68% of the total N pool (Table 2). The second-most concentrated N species in the Hillcrest sample was NH_4^+, present at 4 μM, comprising 32% of the N pool.

In the monitored spring draining the beef-cattle pasture, spring SpW2, $[NO_3^-]$, and $[N_2O]$ covaried in a statistically significant, inverse fashion (Fig. 3). In contrast, NO_2^-, which is an intermediate denitrification product between NO_3^- and N_2O, apparently did not covary with either of these species, neither visually nor statistically (Fig. 3).

Present at $\leqslant$7 μM, (Table 1), urea N generally was a small fraction of N_{org} in our samples (3–23%; Table 2). One of two samples drawn from NU18, the well located in the beef-cattle pasture, had detectable N^d_{org}; in this sample urea comprised 41% of N^d_{org} (Table 2). In contrast, at the drainage of the beef-cattle pasture downgradient from NU18, spring SpW2, urea represented an average of only 8% of N_{org} (Table 2).

The analytical results for dissolved $[N_2]$ show a N_2 enrichment at all sample locations, relative to water equilibrated with air (Fig. 4). The subsurface-source waters of well NU18 have higher $[N_2]$ than the surface waters collected from the wetland and spring SpW2 $[N_2]$ is intermediate between that of NU18 and the wetland.

Values of $[H_2O_2]$ at spring SpW2 were 4 nM for each of two sampling rounds (Table 3). These values are lower than the 20 nM we had estimated in our earlier work (Washington et al., 2004) based on a mean of values reported for groundwater in Holm et al. (1987). We reported upon most of the other analytes shown in Table 3 in our earlier work (Washington et al., 2004) and, without exception, these new data fall in the same general range as our earlier work.

5. Discussion

5.1. Confirmation that the O_2/H_2O_2 redox couple approaches equilibrium with several N and Fe couples

In our earlier work (Washington et al., 2004), we hypothesized that the O_2/H_2O_2 redox couple approaches equilibrium with several N and Fe couples based on measured values of $[O_2]$ and pH, and a $[H_2O_2]$ estimated to be the mean of several groundwater values reported in Holm et al. (1987), 20 nM. Our actual measured values were a little lower, 4 nM (Table 3). When our measured

Table 1
Analytical data

Date	$[NO_3^-]$ (mM)		Dissolved $[N_{org}]$ (μM)		[Urea-N] (μM)		$[N_2O]$ (μM)		$[NO_2^-]$ (μM)		$[NH_4^+]$ (μM)		Partculate N_{org} (μM)		Non-urease active $[N_{org}]$[a] (μM)		$[C_{org}]$ (μM)		$[O_2]$ (μM)	
	Mean	SD	Mean	SD	Mean	SD	Mean	SD	Mean	SD	Mean	SD	Mean	SD	Mean	SD	Mean	SD	Mean	SD
Spring W2																				
07/11/2001	0.49	0.03	41	4							0.6	0.2	<10				50	1		
09/26/2001	0.37	0.02	29	3					0.21	0.04	0.5	0.4	<10				40	1	0.17	0.003
10/16/2001	0.33	0.02	26	2					0.18	0.04	<3		<10				23	2	0.25	0.02
11/29/2001	0.30	0.02	23	2	2.8	0.3			0.57	0.00	<0.6		<10		20	4	15	1	0.22	0.009
12/06/2001	0.30	0.02	21	2	1.0	0.1							<10		20	4	20	2		
01/23/2002	0.41	0.02	42	4					0.21	0.00	<0.6		14	1			63	1	0.24	0.007
03/19/2002	0.36	0.02	28	3	1.3	0.2	0.37	0.02	0.21	0.04	<3		<10		27	6	20	0	0.27	0.004
06/03/2002	0.36	0.02	27	2			0.96	0.11	<0.2		<0.4		11	1			14	1	0.15	0.002
06/25/2002	0.32	0.02	32	3	7.4	0.9	2.17	0.14	0.25	0.04	<0.6		<10		25	5	44	3	0.20	0.002
07/29/2002	0.31	0.02	35	3	5.9	0.7	1.20	0.02	0.21	0.02	0.6	0.0	<10		29	6	55	1	0.16	0.006
10/02/2002	0.36	0.02	43	4	4.0	0.5	0.80	0.04	<0.2		<0.6		<10		39	8	38	2	0.17	0.001
11/20/2002	0.72	0.04	79	7	2.7	0.3	0.50	0.03	0.25	0.05	<0.6		<10		76	16	37	1	0.22	0.004
12/18/2002	0.45	0.03	46	4	1.3	0.2	0.38	0.02	0.36	0.00	0.7	0.2	<10		45	9	28	2	0.22	0.004
01/07/2003	0.49	0.03	49	4	2.5	0.3	0.38	0.04	0.35	0.02	<0.6		<10		47	10	41	3	0.22	0.007
02/24/2003	0.48	0.03	58	5	3.1	0.4	0.17	0.01	0.24	0.04	<0.6		<10		54	11	51	2		
04/03/2003	0.46	0.03	25	2			0.38	0.01	0.29	0.00	<0.6		19	2			41	2	0.23	0.006
05/12/2003	0.44	0.03	38	3			0.51	0.03	0.25	0.00	<0.6		<10				16	1	0.18	0.02
06/05/2003	0.42	0.03	32	3	1.1	0.1	0.41	0.00	0.21	0.00	0.8	0.1	<10		31	7	220	5	0.22	0.005
NW Spring																				
02/26/2002	0.10	0.01	<14				0.16	0.00	0.29	0.07	<3		<10				22	2	0.20	0.002
03/07/2002							0.15	0.01	0.39	0.04	<3								0.18	
Well NU18																				
05/08/2002	0.24	0.01	<14		1.2	0.1	5.27	0.26	0.71	0.07	<4		<10		3	1	240	2	0.08	0.001
06/05/2002	0.27	0.02	~11	1	4.6	0.6	1.03	0.10	0.28	0.02	<4		<10		7	1	96	1	0.19	0.008
Hillcrest Well																				
07/23/2002			9	1	2.0	0.2	0.01	0.01			4.3	0.0	<10		7	1	49	2	<0.009	

[a] Non-urease active N_{org} is $[N_{org}]$–[Urea-N].

Table 2
Ratios

Date	Molar fraction of total dissolved N					Molar urea N/N_{org}	Molar C_{org}/N_{org}
	NO_3^-	N_{org}	NO_2^-	N_2O	NH_4^+		
Spring W2							
07/11/2001	0.92	0.08	0.0000	0.0000	0.0011		1.22
09/26/2001	0.93	0.07	0.0005	0.0000	0.0012		1.35
10/16/2001	0.93	0.07	0.0005	0.0000	0.0000		0.88
11/29/2001	0.93	0.07	0.0017	0.0000	0.0000	0.12	0.63
12/06/2001	0.94	0.06	0.0000	0.0000	0.0000	0.05	0.97
01/23/2002	0.91	0.09	0.0005	0.0000	0.0000		1.53
03/19/2002	0.93	0.07	0.0006	0.0010	0.0000	0.05	0.69
06/03/2002	0.93	0.07	0.0000	0.0025	0.0000		0.52
06/25/2002	0.91	0.09	0.0007	0.0062	0.0000	0.23	1.37
07/29/2002	0.90	0.10	0.0006	0.0034	0.0017	0.17	1.60
10/02/2002	0.90	0.10	0.0000	0.0020	0.0000	0.09	0.89
11/20/2002	0.90	0.10	0.0003	0.0006	0.0000	0.03	0.47
12/18/2002	0.91	0.09	0.0007	0.0008	0.0014	0.03	0.61
01/07/2003	0.91	0.09	0.0006	0.0007	0.0000	0.05	0.84
02/24/2003	0.89	0.11	0.0004	0.0003	0.0000	0.05	0.89
04/03/2003	0.95	0.05	0.0006	0.0008	0.0000		1.68
05/12/2003	0.92	0.08	0.0005	0.0011	0.0000		0.41
06/05/2003	0.93	0.07	0.0005	0.0009	0.0018	0.03	6.70
NW Spring							
05/08/2002	0.96		0.0028	0.0016	0.0000		>1.6
Well NU18							
05/08/2002	0.98		0.0029	0.0213	0.0000		>17
06/05/2002	0.96	0.04	0.0010	0.0037	0.0000	0.41	8.60
Hillcrest Well							
07/23/2002	0.00	0.68	0.0000	0.0009	0.32	0.22	5.46

values are used to calculate pe_{O_2/H_2O_2} using (Washington et al., 2004):

$$pe(O_2/H_2O_2) = (26.32 + \log\ a_{O_2} - \log\ a_{H_2O_2} - 2pH)/2 \quad (5)$$

the resulting potentials plot closer to equality with $pe_{NO_3^-/NO_2^-}$ than we had estimated in our earlier work (Fig. 5 herein vs. Fig. 1A in Washington et al., 2004). The observation that pe_{O_2/H_2O_2} nearly equates with $pe_{NO_3^-/NO_2^-}$ supports that multiple oxidants can be subject to reduction simultaneously. In this case, the O_2/H_2O_2 and NO_3^-/NO_2^- couples apparently are mutually buffering each other's reductive consumption.

Because there has been a longstanding controversy regarding whether O_2 in aqueous environmental systems mostly is reduced to the intermediate H_2O_2 or directly to H_2O (Drever, 1988), this confirmation that O_2/H_2O_2 is closely consistent with a number of other couples over several years of observation at a single site (Fig. 5) and at several locations (Washington et al., 2004) is important support that O_2 reduction generally does proceed through the H_2O_2 intermediate. That O_2 reduction generally is a two-step process, $O_2 \rightarrow H_2O_2 \rightarrow H_2O$, also is corroborated by the steady increase in fluorescence observed for samples stored in sunlight during H_2O_2 analysis, apparently reflecting the ingrowth of H_2O_2 (Section 3.5 of this paper).

5.2. Mineralization of urea to near partial equilibrium with dissolved O_2 reduction

Ammonification of urea to NH_4^+ is mediated by the urease enzyme and is thermodynamically spontaneous for most environmental conditions. In detail, urease appears to catalyze urea hydrolysis to the intermediate product ammonium carbamate ($H_2NCOONH_4$ which quickly reacts abiotically to form NH_4^+ under most environmental conditions (Jespersen, 1975).

When N is not the limiting nutrient under oxidizing conditions, such as at the N-rich spring SpW2, large fractions of ammonification-formed NH_4^+ can be expected to be subject to nitrification. Under these conditions, ammonification and nitrification comprise a closely coupled, two-step mineralization process that can be represented as:

$$CO(NH_2)_2 + 6H_2O \rightarrow 2NO_2^- + 14H^+ + 12e^- + H_2CO_3 \quad (6)$$

Using free energies of formation from Brock et al. (1994), for Eq. (6), $\log K = -168.53$. Solving for calculated redox potential, $pe_{NO_2^-/CO(NH_2)_2}$ is expressed as:

$$pe_{NO_2^-/CO(NH_2)_2} = (168.53 + \log\ a_{H_2CO_3} + 2\log\ a_{NO_2^-} - 14pH - \log\ a_{CO(NH_2)_2})/12 \quad (7)$$

Applying N data reported herein (Table 1), and H_2CO_3 and pH data as reported in Washington et al. (2004) to

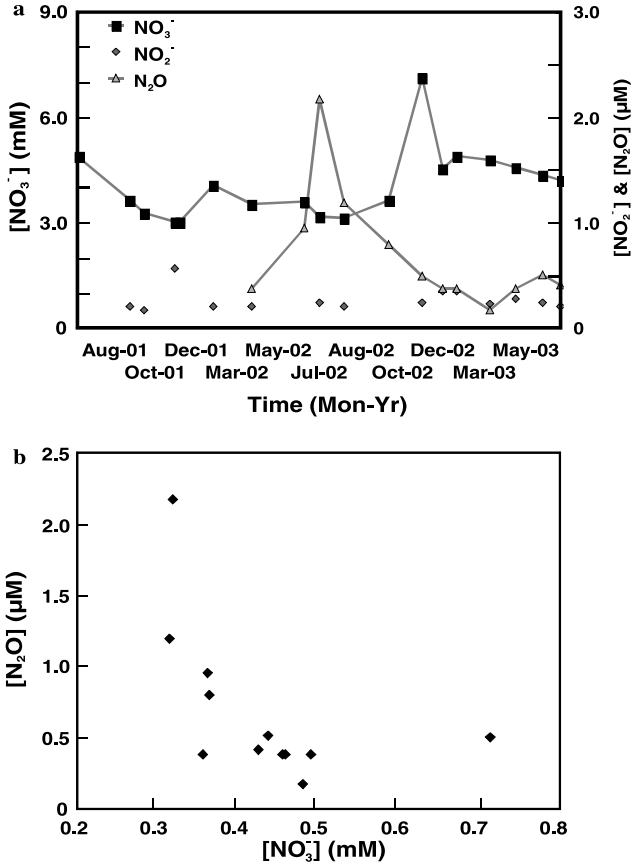

Fig. 3. (a) $[NO_3^-]$, $[NO_2^-]$, and $[N_2O]$ vs time in spring SpW2 water. With a correlation coefficient between the log-transformed $[NO_3^-]$ and $[N_2O]$ of $r^2 = 0.36$, these solutes are inversely correlated at $P = 0.05$ (10 df). However, $[NO_2^-]$ is not significantly related to either of the other solutes. (b) $[N_2O]$ vs. $[NO_3^-]$, depicting inverse relationship in spring SpW2.

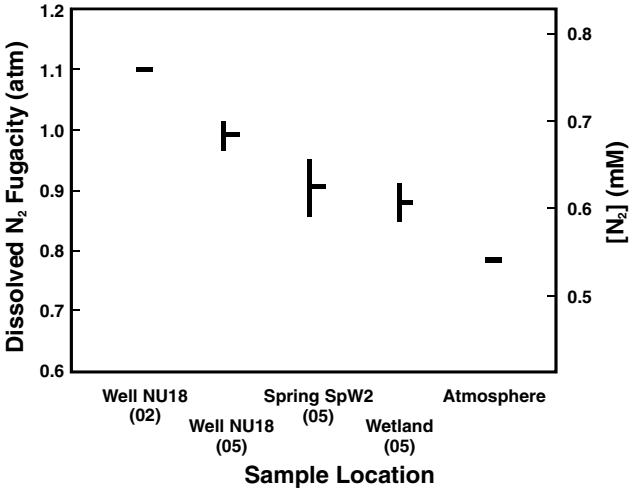

Fig. 4. N_2 fugucity f_{N_2} by sample location designated by sample source and sampling year. Symbols represent mean, plus and minus one standard deviation. All sample locations had f_{N_2} in excess of atmospheric, 0.78 atm, depicted above for reference. Screened through a saturated aquifer thickness of about 10 m, the hydrostatic pressure in well NU18 was sufficient to allow f_{N_2} of equal to and in excess of 1 atm for the two sampling rounds. Samples from spring SpW2 and the wetland into which it drained had 0.78 atm $< f_{N_2} <$ 1.0 atm. Whereas the high f_{N_2} of well NU18 and spring SpW2 could reflect contributions of 'excess air' from bubble entrainment in recharge areas as well as denitrification, the wetland sample was collected from surface-water shoals and, thus, likely is a consequence of denitrification alone.

Eq. (7), $pe_{NO_2^-/CO(NH_2)_2}$ for spring SpW2 is depicted in Fig. 5 along with pe values for other analytes. For these calculations, the activity of NO_2^- was calculated from concentration using the extended Debye–Huckel equation (Washington et al., 2004) and, as neutral species, H_2CO_3 and urea were assumed to have activity coefficients of unity. Fig. 5 shows that values of $pe_{NO_2^-/CO(NH_2)_2}$ remain stable through time like all other depicted couples and are positioned at the bottom of the upper pe cluster defined by most other calculated N pe values, Fe pe values and pe_{O_2/H_2O_2}.

With $pe_{NO_2^-/CO(NH_2)_2}$ generally being <4 pe units from pe_{O_2/H_2O_2}, these couples are close to mutual equilibrium compared to: (1) the stability field for water which is about 21 pe units; and (2) the free energy that microbes typically leave untapped due to constraints required to fuel their metabolism. According to Thauer et al. (1977), microbes typically leave about −2.8 kcal/(mol H_2) unused or, more generally, −2.8 kcal/2 mol e^- (this is a conventional basis upon which biochemical thermodynamics are reported; Brock et al., 1994). If we treat the energy gap between $pe_{NO_2^-/CO(NH_2)_2}$ and pe_{O_2/H_2O_2} (Fig. 5) as though it results from the reaction of urea with dissolved O_2 to produce NO_2^- and H_2O_2, the reaction can be given as:

$$CO(NH_2)_2 + 6O_2 + 6H_2O \rightarrow 2NO_2^- + H_2CO_3 + 2H^+ + 6H_2O_2 \quad (8)$$

for which the free energy (ΔG_{urea}) is given by:

$$\Delta G_{urea} = \Delta G^o_{urea} + RT \ln \frac{a^2_{NO_2^-} a^2_{H^+} a_{H_2CO_3} a^6_{H_2O_2}}{a_{CO(NH_2)_2} a^6_{O_2}}, \quad (9)$$

where ΔG^o_{urea} is the standard state free energy, R is the universal gas constant, T is temperature in kelvin, and a_x is activity for species x. Using the thermodynamic data represented by Eqs. (7) and (9), the standard-state free energy is $\Delta G^o_{urea} = 14.04$ kcal/mol. Using mean values for species from spring SpW2 (Table 1 and Washington et al., 2004), calculating an activity coefficient for NO_2^- using the Extended Debye–Huckel Eqn. (Stumm and Morgan, 1996), and assuming activity coefficients of unity for neutral species, the calculated energy gap for Eq. (9) is −44 kcal/mol urea or −7.3 kcal/2 mol e^-, about 2.6-times the maximum biological endpoint. Hence, the energetic gap depicted between $pe_{NO_2^-/CO(NH_2)_2}$ and pe_{O_2/H_2O_2} (Fig. 5) is on the order of, or slightly larger than, that typically left unused in microbial processes that are not reactant-concentration limited.

In Washington et al. (2004), we depicted evidence, reproduced here as Fig. 6, that the approach of redox-active solutes toward equilibrium with their dominant complementary reactants is a function of reactant concentration, where we define 'dominant complementary reactant' as the most concentrated oxidant of a higher-potential

Table 3
2005 Analytical data

Parameter	June 16, 2005		June 23, 2005	
	Mean	SD	Mean	SD
Flow rate (L/min)	28.7	0.5	38.3	0.5
Spec. Cond (μS)	85.6	0.7	94.5	0.4
pH (SU)	5.16	0.01	5.01	0.01
Temperature (C)	17.7	0	18.3	0.04
$[O_2]$ (mM)	0.21	0.005	0.15	0.005
$[H_2O_2]$ (nM)	4	0.8	4	1
$[H_2]$ (nM)	0.31	0.08	0.86	0.11
Alk. Equiv. $[HOO_3^-]$ (mM)	<0.2		<0.2	
$[H_2CO_3]$ (mM)	0.92	0.006	1.3	0.008
$[CH_4]$ (nM)	<7		<7	
$[C_{org}]$ (MM)	0.39	36	32	18
$[NO_3^-]$ (mM)	0.24	0.001	0.41	0.001
$[NO_2^-]$ (μM)	0.33	0.04	0.4	0.04
$[N_2O]$ (μM)	0.22	0.002	0.32	0.002
$[NH_{4-}]$ (μM)	0.83	0.22	1.3	0.39
$[N_{org}]$ (μM)	0.31	9	29	3
Partic. $[N_{org}]$ (μM)	<10		<10	
[Urea-N] (μM)	<0.9		0.55	0.47
$[N_2]$ (μM)	0.62	0.02	0.63	0.04
$[SO_4^-]$ (μM)	17	0.6	21	0.1
$[H_2S]$ (nM)	<30		90	10
[Fe(ll)] (μM)	3.7	0.4	2.5	2.0
[Fe(lll)] (μM)	4.6	2.3	2.4	1.9
$[Cl^-]$ (mM)	0.24	0.001	0.26	0.001

couple for each reduced solute and the most concentrated reductant of a lower-potential couple for each oxidized solute (Washington et al., 2004). The significance of this definition is rooted in the fact that solutes often vary in concentrations by orders of magnitude among each other in environmental systems. Such broad variability in solute concentrations is inferred to mirror roughly each solute's relative capacity to buffer the redox potential of its couple and, hence, its capacity to define the effective equilibrium endpoint toward which other potential reactants are drawn. In systems having two or more reactants of nearly equal concentrations, factors other than relative concentration are likely to control which is the true 'dominant complementary reactant.' At spring SpW2, the concentrations of NO_3^- and O_2 (Table 1), and the potentials of their couples (Fig. 5), nearly are equal; consequently, with regard to oxidation of reduced solutes, the choice of dominant complementary reactant between NO_3^- and O_2 for lower potential reduced species is arbitrary. In Fig. 6, the approach toward equilibrium between couples is defined as the difference in pe value of each solute from its dominant complementary reactant; in the case of urea, Δpe is the difference in pe value between the urea oxidation reaction and either NO_3^- or O_2 reduction, but conventional thought on the process of urea oxidation has it that O_2 is the dominant complementary oxidant. Regardless, plotting urea on Fig. 6 shows that data for urea → NO_2^- do indeed conform to the pattern of most of our other data.

5.3. Mineralization of N_{org} for energy and near partial equilibrium with dissolved O_2 reduction

Only within the last decade have new analytical techniques allowed definition of the functionality of N_{org}.

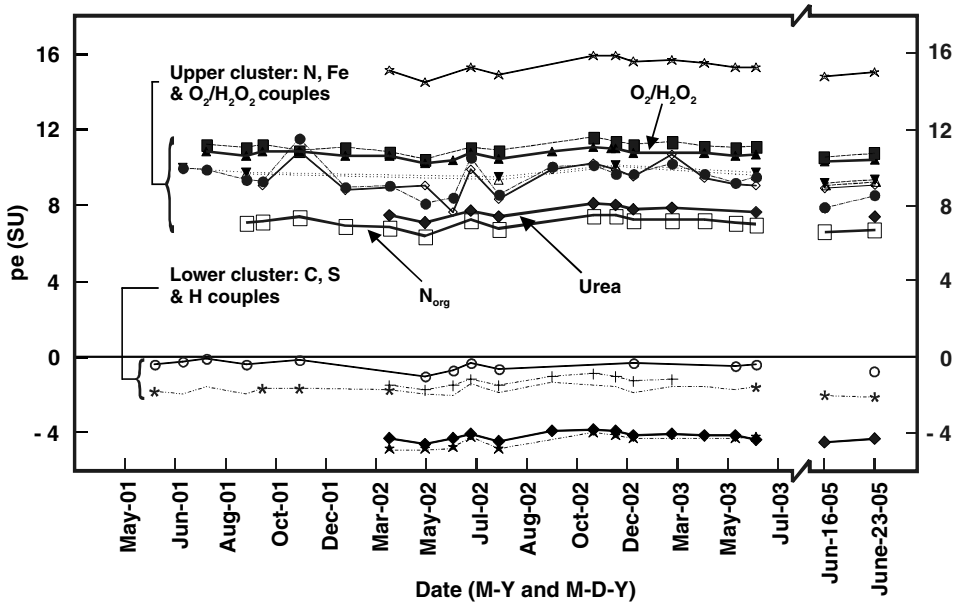

Fig. 5. Calculated redox potential for the mineralization of urea ($pe_{NO_2^-/CO(NH_2)_2}$) and N_{org} ($pe_{NO_2^-/RCONH_2}$), modeled as the amide functional group, vs. time in spring SpW2. Also shown are other calculated redox potentials we have reported previously (Washington et al., 2004). The redox potentials we calculated for urea and N_{org} mineralization to NO_2^- closely approach the upper redox cluster comprised of other N and Fe couples, and the inferred major oxidant of reduced N, $O_2 \rightarrow H_2O_2$. For these data, pe_{O_2/H_2O_2} is calculated from measured data $[O_2]$ and pH, and $[H_2O_2] = 4$ nM, a value that was measured twice at spring SpW2 for the last two sample dates depicted in this figure. The calculated urea, N_{org} and H_2O_2 couples are shown in bold line with symbols of: (♦) $NO_2^-/CO(NH_2)_2$; (□) $NO_2^-/RCONH_2$; (▲) O_2/H_2O_2 . Other depicted symbols are were first reported in Washington et al. (2004) and are shown here for comparison: (▽) O_2/H_2O; (■) NO_3^-/NO_2^-; (☆) NO_2^-/N_2O; (▼) NO_3^-/NH_4^+; (△) NO_2^-/NH_4^+; (●) $Fe(OH)_{3PPT}/Fe^{2+}$; (♦) $Fe(OH)_2^+/Fe^{2+}$; (○) $SO_4^=/H_2S$; + $H_2CO_3^*/CH_4$; (★) $H_2CO_3^*/CO$; (*) H_2O/H_2; (♦) $H_2CO_3^*/C_{org}$.

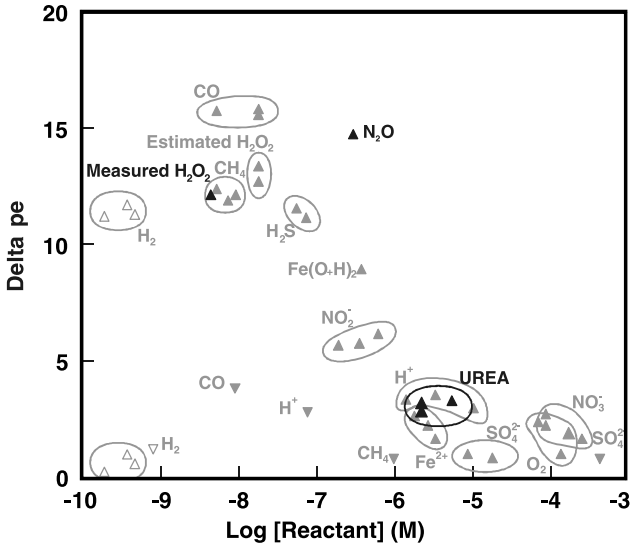

Fig. 6. Δpe from the dominant complementary couple vs log measured reactant concentration, see text for detailed explanation. Lightly shaded data are reproduced from Washington et al. (2004) and the bold data points are newly reported here: urea from samples collected during 2001–2003 and frozen; H_2O_2 and N_2O collected on June 23, 2005 from spring SpW2. Up-pointing triangles depict data for samples having quantifiable O_2, the 3 shallower sample locations. Down-pointing triangles depict data for the deep-source sample that had no quantifiable O_2. At concentrations $>10^{-6}$ M, Δpe consistently is small. At concentrations $<10^{-6}$ M, Δpe trends upward. Present at $\sim10^{-6}$ M, urea is close to equilibrium, that is, Δpe is small. Open symbols are plotted twice due to questions regarding the dominant oxidant, see Washington et al. (2004) for details.

In some of this earliest work, Knicker and Ludemann (1995) examined aged terrestrial organic matter using ^{15}N NMR and discovered that, contrary to conventional thought, the majority of N_{org} was present as amide functional groups. Marine organic matter generally is supposed to be generated in the sea under dramatically different conditions than terrestrial organic matter; despite this difference in origins, when McCarthy et al. (1997) applied ^{15}N NMR to marine organic matter, they discovered that marine N_{org} also is present dominantly as amide groups. Still more recently, Vairavamurthy and Wang (2002) used K-edge XANES spectroscopy to determine that riverine N_{org} also dominantly is present as amides.

Because amides generally are considered to be environmentally labile moieties (Vairavamurthy and Wang, 2002), these recent discoveries that N_{org} is present dominantly as amides has struck many as incongruous with the common observation that a significant fraction of N_{org} is quite persistent. A couple of theories have been proposed to account for the seemingly refractory nature of these N_{org} amide groups: (i) adsorption of labile materials to mineral surfaces that are inaccessible to microbial enzymatic attack (Mayer, 1995); and (ii) encapsulation of labile materials in resistant fractions (Zang et al., 2000).

While these theories differ in their mode of action, they share a common underpinning in that they propose conditions that might slow otherwise-fast degradation of the N_{org} amide groups. However, the more fundamental issue remains of whether some fraction of N_{org} might persist, not because it is refractory, but because its couple is near partial equilibrium with its dominant oxidant couple.

At its most elementary, ammonification of N_{org} amides simply is nucleophilic attack by water on the amide bond to produce a carboxyl and NH_4^+:

$$RCONH_2 + H^+ + H_2O \rightarrow RCOOH + NH_4^+, \quad (10)$$

where R is an organic molecule. When the ammonification represented in Eq. (10) is coupled to nitrification, mineralization of N_{org} amides can be represented as:

$$2RCONH_2 + 6H_2O \rightarrow 2NO_2^- + 14H^+ + 12e^- + 2RCOOH \quad (11)$$

Expressed in this form, Eq. (11) is functionally equivalent to the mineralization of urea as shown in Eq. (6) in that, for each reaction, two amine–carboxyl bonds are cleaved, two hydroxyl–carboxyl bonds are formed and all other bond transitions are identical. As such, the energetics of Eq. (11) can be expected to be closely similar to those of Eq. (6) and, consequently, mineralization of N_{org} might be approximated by modeling N_{org} as urea. Normalizing Eq. (11) to a single amide functional group and approximating the free-energy of reaction for N_{org} with the urea data, $\log K \simeq 1/2(-168.53) = -84.27$ and $pe_{NO_2^-/RCONH_2}$ can be approximated as:

$$pe_{NO_2^-/RCONH_2} = (84.27 + \log a_{RCOOH} + \log a_{NO_2^-} - 7pH - \log a_{RCONH_2})/6 \quad (12)$$

In Eq. (12), NO_2^- and pH are measured, and $RCONH_2$ can be approximated by N_{org}. The value of the organic carboxyl group is not directly represented by any of our analytical quantities. If both RCOOH and NO_2^- were products solely of nitrification via Eq. (12), and neither reacted further, then the stoichiometric equivalence of RCOOH with NO_2^- would render $[NO_2^-]$ a flawless estimate of [RCOOH]. In complex natural systems, however, both RCOOH and NO_2^- serve as reactants and products in numerous other reactions. Nevertheless, $[RCOOH] \simeq [NO_2^-]$ is the best approximation we have for our data. Furthermore, the effect of errors from applying this approximation are minimized in Eq. (12) by taking the log of [RCOOH] and dividing the entire quantity by six. Hence, we approximate Eq. (12) as:

$$pe_{NO_2^-/RCONH_2} \simeq (84.27 + 2\log a_{NO_2^-} - 7pH - \log a_{RCONH_2})/6 \quad (13)$$

Assuming an activity coefficient for the amide functional groups of unity, values of $pe_{NO_2^-/RCONH_2}$ calculated from Eq. (13) are plotted in Fig. 5. These values for $pe_{NO_2^-/RCONH_2}$ can be seen to closely mimic those calculated for $pe_{NO_2^-/CO(NH_2)_2}$; while this pattern is to be expected because of the large number of common variables used to calculate these potentials, it also is consistent with the idea that amide moieties on complex organic molecules behave

similarly to those on urea, which we maintain is a reasonable proposition as well. Furthermore, $pe_{NO_2^-/RCONH_2}$ and $pe_{NO_2^-/CO(NH_2)_2}$ define the bottom of the upper cluster of redox values comprised of other N pe values, Fe pe values and pe_{O_2/H_2O_2} values. This observation is consistent with the idea that, in N-rich settings, organic amide moieties commonly can approach partial equilibrium with the dominant oxidant in environmental systems.

Because we analyzed $[N_{org}]$ on an atomic basis, as opposed to molecular, we do not have the necessary information to plot these data on the molecular concentration scale of the *x* axis in Fig. 6. To the extent our approximation of $pe_{NO_2^-/RCONH_2}$ is correct (Fig. 5), its deviation from the dominant complementary reactants and the relationship depicted in Fig. 6 implies that our measured atomic concentration of $[N_{org}] \sim 10^{-5}$ M equates to a molecular concentration of about 10^{-6} M. In turn, this estimate suggests a mean N molecular size of about N_{10}. Using an analogous approach for C_{org}, our measured atomic concentration of $[C_{org}] \sim 10^{-5}$ M equated to a molecular concentration of about 10^{-7} to 10^{-8} M (Washington et al., 2004). To the extent these approximations are valid, the closer approach of N_{org} to its dominant complementary reactant than C_{org} with its dominant complementary reactant suggests that N_{org} is preferentially concentrated in the smallest organic molecular fractions.

5.4. Modes of accumulation of excess N_2 and its possible effervescence

There are two modes by which subsurface waters have been shown to accumulate $[N_2]$ in excess of that for equilibration with air: (1) denitrification; and (2) percolating waters entrap air at and near the water table, and, as the waters advect downward with the entrained bubbles, dissolve the bubbles under the influence of the increasing hydrostatic pressure (Kipfer et al., 2002).

Among the three N_2 sample locations, the well, NU18, had the highest f_{N_2}, with $f_{N_2} \approx 1.0$ atm (Fig. 4) when we sampled during unusually wet conditions in 2005 and $f_{N_2} \approx 1.1$ atm when we sampled during drought conditions in 2002. Had the waters entered the system equilibrated with the atmospheric value of $f_{N_2} = 0.78$ atm, the water entering the subsurface system would have had dissolved $[N_2] = 0.54$ mM. Consequently, the subsurface waters from which the samples (Fig. 4) were drawn are at least partially closed with respect to the atmosphere and the differences (0.69–0.54 mM) to (0.76–0.54 mM) = 0.15–0.22 mM of excess dissolved N_2 had accumulated in well NU18 by denitrification of NO_3^- and/or NO_2^-, and/or by air entrapment.

In contrast to subsurface waters, surface waters usually are observed to contain dissolved-gas fugacities that are near equilibrium with air (Kipfer et al., 2002). As such, the observation of the high $[N_2]$ in the water collected from the wetland shoals (Fig. 4), 70-m downstream of spring SpW2 (Fig. 4), supports the presence of an active source of N_2 to this water, i.e., denitrification. In turn, this suggests that at least some of the excess N_2 observed in well NU18 and spring SpW2 is from denitrification.

Since the $f_{N_2} \approx 1.1$ atm we measured in well NU18 exceeded the total atmospheric pressure, depths below the water table, for which the hydrostatic pressure was less than 1.1 atm, were supersaturated with respect to N_2. As such, N_2 might well have been exsolving from solution in the aquifer discharge zone near spring SpW2 at depths of <100 cm below the water table, where $P_{hydrostatic} < 1.1$ atm, if bubble-nucleation energy was overcome and if the exsolved bubbles could find macropores in which they were able to migrate upward.

The terminal step of denitrification commonly is reported as $N_2O \rightarrow N_2$ (Betlach and Tiedje, 1981), for which the balanced reaction can be written:

$$N_2O + 2H^+ + 2e^- \rightarrow N_2 + H_2O \quad (14)$$

Using thermodynamic data from Bethke (1998):

$$pe_{N_2O/N_2} = (59.899 + \log a_{N_2O} - \log a_{N_2} - 2pH)/2 \quad (15)$$

Applying data reported herein (Table 1), the deviation of pe_{N_2O/N_2} from its dominant complementary couple, $pe_{Fe(OH)_{3ppt}/Fe^{2+}}$, is plotted in Fig. 6, labeled with its reactant, N_2O, the anomalous value of this couple is obvious. Based on the fugacity of the samples exceeding 0.78 atm and the stoichiometry of Eq. (14), the unusually high potential for this couple further supports that exsolution of the volatile product, N_2, takes place in this setting.

5.5. Denitrification as a possible cause of NO_3^- and N_2O covariation

The temporal variation of N solutes in spring SpW2 is notable because of the concomitant, inverse variation in $[NO_3^-]$ and $[N_2O]$ (Fig. 3). Solute concentration changes might be expected as a function of variability in rate of application of manure, the ultimate source of the N, or variability in recharge affecting transport or dilution. However, these changes in source term seem likely to affect parallel, as opposed to the observed inverse, changes in all the N solutes or, perhaps, a change in one solute with little effect on the others because of slow solute-degradation rates. Accordingly, simple change in source term seems to be an unlikely cause for the observed pattern of concomitant, inverse variation in $[NO_3^-]$ and $[N_2O]$.

As described above, the observed excess dissolved N_2 in samples from well NU18, spring SpW2, and the surficial wetland waters suggests that denitrification is taking place in the aquifer system. When a transformation process proceeds through a series of intermediate products, as with denitrification, the product ratios vary systematically with reaction progress, both in static systems (Friedlander et al., 1981) and in flow-through systems (Washington and Cameron, 2001). Consequently, a possible cause for the inverse correlation between NO_3^- and N_2O (Fig. 3) is variation in the degree of denitrification progress, e.g., as a result of seasonal

variation in groundwater flow rate affecting residence time or temperature affecting reaction rate.

As is true of most enzymatically driven reactions, the actual rates of denitrification vary drastically with environmental variables such as temperature and [C_{org}]; however, the general systematics of sequential ingrowth and decay is a common factor for the process. Fig. 7 depicts the calculated product concentrations during denitrification in a closed chemical system, relative to the time-zero concentration of the parent NO_3^-, as a function of reaction progress based on Michaelis–Menten half-saturation constants reported in Betlach and Tiedje (1981). This figure illustrates how small variations in reaction progress alter the relative proportions of reactants and products in a closed system. In particular, the reaction-progress period of ~0.05 to ~0.1 is an interval during which [NO_3^-] is decreasing, [N_2O] is increasing and [NO_2^-], near its concentration apex, is roughly invariant, similar to the pattern observed in spring SpW2 data (Fig. 3).

Low [NO_3^-] and high [N_2O] generally occurred in spring SpW2 during the summer, and high [NO_3^-] and low [N_2O] occurred during autumn through spring. Flow rate from spring SpW2 was slower during the summer than at other times (Washington et al., 2004) and this pattern might cause the observed patterns in [NO_3^-] and [N_2O] because lower flow rates should cause longer residence times leading to more complete denitrification. There is statistical support for this hypothesis in that log-transformed flow rate is significantly correlated with log transformed [NO_3^-] ($P < 0.05$) and log-transformed [N_2O] ($P < 0.01$). Water temperatures were warmer in the summer than at other times (Washington et al., 2004) and warm temperatures would favor increased reaction rates, thus potentially causing the observed patterns in [NO_3^-] and [N_2O] as well. Testing this hypothesis statistically, log-transformed temperature is significantly correlated with log-transformed [N_2O] ($P < 0.01$), but is not significantly correlated with log-transformed [NO_3^-], so the statistical evidence for this hypothesis is not as strong as that for changes in flow rate as a causative factor of the observed [NO_3^-] and [N_2O] patterns. Taken together, these observations suggest that variability in flow rate at spring SpW2 caused the issuing waters to have undergone varying degrees of denitrification progress.

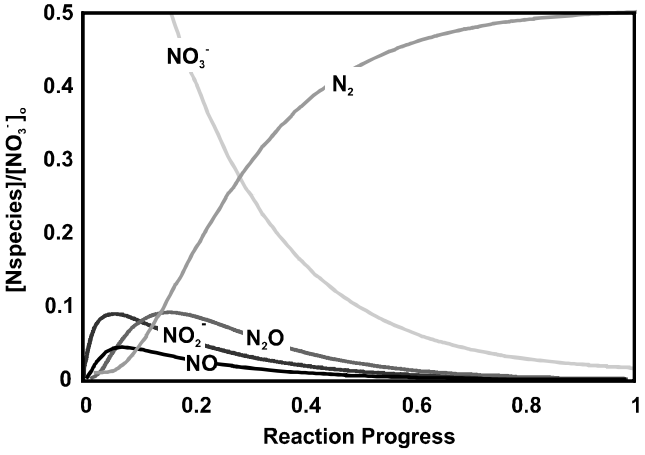

Fig. 7. Ratio of N-species concentration to initial [NO_3^-] vs reaction progress for the denitrification reaction sequence of $NO_3^- \rightarrow NO_2^- \rightarrow NO \rightarrow N_2O \rightarrow N_2$ using the Michaelis–Menten half-saturation constants for *Flavobacterium* as reported in Betlach and Tiedje (1981). For much of the reaction period from ~0.05 to ~0.1, increasing progress diminishes [NO_3^-] at the same time as [N_2O] increases and [N_2O^-], near its maximum, remains nearly constant—a qualitatively similar pattern as that observed for spring SpW2. Note that [N_2O] and [N_2] are decreased by half relative to other species to account for reaction stoichiometry. Also note that: (1) the half-saturation constant for NO, which was not reported by Betlach and Tiedje (1981), herein is assumed equal to that of N_2O; and 2) Betlach and Tiedje (1981) did not report Michaelis–Menten maximum velocities (v) which vary dramatically with environmental conditions—to model relative concentrations similar to our data we used $v_{NO_3^-} = 1$, $v_{NO_2^-} = 6$, $v_{NO} = 1$ and $v_{N_2O} = 0.2$.

5.6. C_{org}/N_{org} indicates that the SpW2 aquifer microbial ecosystem is N saturated

Redfield (1934, 1958) found that, through biological assimilation, "biological agencies" control the C_{org}/N_{org} molar ratios typically observed in aqueous systems receiving natural concentrations of N compounds at values of $C_{org}/N_{org} \approx 6.6$. This Redfield ratio for C_{org}/N_{org} contrasts sharply with C_{org}/N_{org} ratios associated with cattle wastes (feces and urine undivided) which ranges from about 36 when fresh to 21 subsequent to aging (Atiyeh et al., 2000; Lekasi et al., 2003), much above the Redfield ratio. Contrasting with the Redfield ratio nearly as sharply, but in the other extreme, the C_{org}/N_{org} of livestock urine is on the order of unity (van Groenigen et al., 2005), much less than the Redfield value.

Spring NWSp, which drains a forested area, and the deep Hillcrest Well, both were selected for sampling to represent the chemistry of area groundwaters that have not been impacted heavily by agriculture and the low [N] observed in both these locations (Table 1) is supportive that they do, indeed, represent such conditions. Because N_{org} was not detected in spring NWSp (Table 1), we can only define the lower limit of the C_{org}/N_{org} ratio for this location using the LOD for N_{org}; for NWSp $C_{org}/N_{org} > 1.4$ (Table 2), a lower-limit ratio that allows a range from well below to above the Redfield value. In the Hillcrest Well, $C_{org}/N_{org} \approx 5.5$ (Table 2), a value that falls just below the Redfield value, suggesting that the C_{org}/N_{org} ratio at this low-agricultural-impact location largely was controlled by assimilative biological processes.

In contrast, the C_{org}/N_{org} values for the sample sites located in a beef-cattle pasture diverge widely from the Redfield ratio. At spring SpW2, the C_{org}/N_{org} molar ratios are low, generally in the range of 0.5–1.7 (Table 2) indicating N_{org} saturation, a condition that is conducive to use of N_{org} to fuel energy production, i.e., dissimilative biological processes. Within the same watershed, but contrasting with the SpW2 data, the C_{org}/N_{org} values for well NU18 were high relative to the Redfield ratio, i.e., 9 and >14 (Table 2). Whereas it seems likely that the wide divergences of the C_{org}/N_{org} ratios for spring SpW2 and well NU18

from the Redfield ratio are related to the sample locations being situated in the beef-cattle pasture, the reason for the still-larger disparity between spring SpW2 and well NU18 remains uncertain. One possible cause for the low C_{org}/N_{org} in spring SpW2 is the habitual congregation of the herd immediately up-slope of SpW2 in pasture area where the groundwater table most-closely approaches the ground surface (Amirtharajah et al., 2002)—it might be that mobile N-rich urine is making its way along the short flow-path to the spring. Regardless, more work is needed if we are to understand the dynamics of C_{org}/N_{org} in agriculturally impacted groundwaters.

6. Conclusions

In the oxic, agriculturally impacted groundwaters we studied, NO_3^- was the dominant fixed-N species, followed by N_{org} and usually relatively trace levels of the other fixed-N species. In the oxic groundwaters showing little to no agricultural impacts, NO_3^- was the dominant fixed-N species, albeit at much lower concentrations than that of the agriculturally impacted waters, followed by relatively trace levels of other fixed-N species. The reducing water showing little to no agricultural impact that we sampled had low concentrations of fixed N relative to the agriculturally impacted waters; among these low concentrations, N_{org} was dominant followed by NH_4^+ and only trace levels of the other fixed-N species.

In oxic, aqueous settings, O_2 is reduced to H_2O_2 rather than directly to H_2O so that potentials for the O_2/H_2O_2 redox couple can approach partial equilibrium with N and Fe couples. In oxic, agriculturally impacted waters: (1) urea can persist because oxidized-N species, NO_3^-, and NO_2^-, are present in sufficient concentrations so that further microbially mediated oxidation of urea is not energetically favorable; and (2) thermodynamic calculations with N_{org}, modeled as the amide bond, suggest that it too might persist in N-rich ecosystems because it has approached near equilibrium with the dominant oxidants in the system.

The observation that N_{org} and urea oxidations approach equilibrium with the reduction of O_2 to H_2O_2 in N-impacted settings extends the pattern we described in Washington et al. (2004) wherein high-concentration redox reactants are close to equilibrium with their dominant complementary reactants and lower concentration reactants, $<10^{-6}$ M in the systems we studied, deviate from equilibrium with their dominant complementary reactant by an amount that is log-linearly proportional to the reactants' concentrations (Fig. 6). Such a pattern describes one with local partial equilibrium (LPE) among high-concentration reactants and concentration reaction-rate limited (CRRL) deviations from equilibrium for low-concentration reactants. In turn, LPE and CRRL conditions among multiple species suggest that these redox reactions are proceeding concomitantly, as opposed to the commonly accepted conceptual model for redox reactions of sequentially in order from highest to lowest energy yield under standard-state conditions.

In addition to extending the application of the combined conceptual models of LPE and CRRL to urea, N_{org} and H_2O_2, we also have identified two exceptions to the pattern manifested by these other reactants: (1) $N_2O \rightarrow N_2$, presumably due at least partially to exsolution of high-fugacity N_2 at high rates relative to the CRRL reduction of N_2O; and (2) $H_2 \rightarrow H^+$, for reasons that are unclear, but might be related to the unique role of H_2 in fermentation or H^+ in acid-base reactions. Nevertheless, the LPE and CRRL models clearly are applicable to multiple redox-active solutes in environmental systems. As such, the LPE and CRRL models show potential to enable estimation of the distribution of redox-active couples and solutes in environmental systems. In fact, the redox couples appear to be remarkably stable (Fig. 5). On the other hand, the LPE and CRRL models seem likely to estimate solute concentrations only with order-of-magnitude-type precision owing to the natural-logarithm functional relation between free energy and reactant/product concentrations (e.g., Eq. (9)).

Acknowledgments

We thank Stephen Norris for help with field efforts. We thank Solvay Chemicals, Inc. for giving us certified H_2O_2. We thank Robert Swank, Vladimir Samarkin, anonymous reviewers and associate editor Michael Machesky for helpful reviews. This research was funded by the USEPA and the USDA-ARS. This paper has been reviewed and approved for publication per USEPA and USDA internal publication approval processes. It may not, however, reflect official policy of the agencies. Mention of a trademark, warranty, proprietary product or vendor does not constitute a guarantee by the USEPA or the USDA, and does not imply approval or recommendation of the product or vendor to the exclusion of others that may be suitable. All programs and services of the USEPA and the USDA are offered on a non-discriminatory basis without regard to race, color, national origin, religion, sex, age, marital status, or handicap.

Associate editor: Michael L. Machesky

References

Aiken, G.R., McKnight, D.M., Wershaw, R.L., MacCarthy, P., 1985. *Humic Substances in Soil, Sediment, and Water*. Wiley-Interscience, New York.

Amirtharajah, A., Young, M.H., Pennell, K.D., Steiner, J.L., Fisher, D.S., Endale, D.M., 2002. *Field Transport of Cryptosporidium Surrogate in a Grazed Catchment*. AWWA Research Foundation.

Appelo, C.A.J., Postma, D., 1996. *Geochemistry Groundwater and Pollution*. A.A. Balkema.

Atiyeh, R., Dominguez, J., Subler, S., Edwards, C., 2000. Changes in biochemical properties of cow manure during processing by earthworms (Eisenia andrei, Bouche) and the effects on seedling growth. *Pedobiologia* **44** (6), 709–724.

Bethke, C.M., 1998. *The Geochemist's Workbench*. University of Illinois.

Betlach, M.R., Tiedje, J.M., 1981. Kinetic explanation for accumulation of nitrite, nitric oxide, and nitrous oxide during bacterial denitrification. *Appl. Environ. Microbiol.* **42** (6), 1074–1084.

Bohlke, J., Denver, J., 1995. Combined use of groundwater dating, chemical, and isotopic analyses to resolve the history and fate of nitrate contamination in two agricultural watersheds, Atlantic coastal plain, Maryland. *Water Resour. Res.* **31** (9), 2319–2339.

Brock, T.D., Madigan, M.T., Martinko, J.M., Parker, J., 1994. *Biology of Microorganisms*. Prentice Hall, Englewood Cliffs, NJ.

Bronk, D.A., Lomas, M.W., Glibert, P.M., Schukert, K.J., Sanderson, M.P., 2000. Total dissolved nitrogen analysis: comparisons between the persulfate, uv and high temperature oxidation methods. *Mar. Chem.* **69**, 163–178.

Clesceri, L., Greenberg, A., Eaton, A., 1998. *Standard Methods for the Examination of Water and Wastewater*. American Public Health Association, New York.

David, M., Gentry, L., Kovacic, D., Smith, K., 1997. Nitrogen balance in and export from an agricultural watershed. *J. Environ. Qual.* **26**, 1038–1048.

Desimone, L., Howes, B., 1996. Denitrification and nitrogen transport in a coastal aquifer receiving wastewater discharge. *Environ. Sci. Technol.* **30** (4), 1152–1162.

Drever, J.I., 1988. *The Geochemistry of Natural Waters*. Prentice Hall.

Driscoll, F.G., 1989. *Groundwater and Wells*. Johnson Filtration Systems, Inc.

Eaton, A., Clesceri, L., Greenberg, A., 1995. *Standard Methods for the Examination of Water and Wastewater*. American Public Health Association, New York.

Friedlander, G., Kennedy, J.W., Macias, E.S., Miller, J.M., 1981. *Nuclear and Radiochemistry*. Wiley, New York.

Goolsby, D.A., 2000. Mississippi basin nitrogen flux believed to cause Gulf Hypoxia. *EOS* **81** (29), 321–327.

Herut, B., Shoham-Frider, E., Kress, N., Fiedler, U., Angel, D.L., 1998. Hydrogen peroxide production rates in clean and polluted coastal marine waters of the Mediterranean, Red and Baltic seas. *Mar. Pollut. Bull.* **36** (12), 994–1003.

Holm, T., George, G., Barcelona, M., 1987. Fluorometric determination of hydrogen peroxide in groundwater. *Anal. Chem.* **59**, 582.

Jespersen, N.D., 1975. A thermochemical study of the hydrolysis of urea by urease. *J. Am. Chem. Soc.* **97** (7), 1662–1667.

Kipfer, R., Aeschback-Hertig, W., Peeters, F., Stute, M., 2002. Noble gases in lakes and ground waters. In: Porcelli, D., Ballentine, C., Wieler, R. (Eds.), *Noble Gases in Geochemistry and Cosmochemistry*, Vol. 47. Geochemical Society & Mineralogical Society of America, pp. 615–700.

Knicker, H., Ludemann, H.-D., 1995. N-15 and C-13 CPMAS and solution NMR studies of N-15 enriched plant material during 600 days of microbial degradation. *Org. Geochem.* **23** (4), 329–341.

Korom, S., 1992. Natural denitrification in the saturated zone: a review. *Water Resour. Res.* **28** (6), 1657–1668.

Korom, S., Schlag, A., Schuh, W., Schlag, A., 2005. In situ mesocosms: denitrification in the Elk Valley Aquifer. *Ground Water Monit. Remediation* **25** (1), 79–89.

Lekasi, J., Tanner, J., Kimani, S., Harris, P., 2003. Cattle manure quality in Maragua District, Central Kenya: effect of management practices and development of simple methods of assessment. *Agric. Ecosyst. Environ.* **94**, 289–298.

Maybeck, M., 1982. Carbon, nitrogen, and phosphorus transport by world rivers. *Am. J. Sci.* **282**, 401–450.

Mayer, L.M., 1995. Sedimentary organic matter preservation: an assessment and speculative synthesis—a comment. *Mar. Chem.* **49** (2–3), 123–126.

McCarthy, M., Pratum, T., Hedges, J., Benner, R., 1997. Chemical composition of dissolved organic nitrogen in the ocean. *Nature* **390** (13), 150–154.

McGuire, J.T., Long, D.T., Klug, M.J., Haack, S.K., Hyndman, D.W., 2002. Evaluating behavior of oxygen, nitrate, and sulfate during recharge and quantifying reduction rates in a contaminated aquifer. *Environ. Sci. Technol.* **36**, 2693–2700.

Miller, W.L., Kester, D.R., 1988. Hydrogen peroxide measurement in seawater by (*p*-hydroxyphenyl)acetic acid dimerization. *Anal. Chem.* **60**, 2711–2715.

Muhlherr, I., Hiscock, K., 1998. Nitrous oxide production and consumption in British limestone aquifers. *J. Hydrol.* **211**, 126–139.

Peterson, B.J., Wollheim, W.M., Mulholland, P.J., Webster, J.R., Meyer, J.L., Tank, J.L., Marti, E., Bowden, W.B., Valett, H.M., Hershey, A.E., McDowell, W.H., Dodds, W.K., Hamilton, S.K., Gregory, S., Morrall, D.D., 2001. Control of nitrogen export from watersheds by headwater streams. *Science* **292**, 86–90.

Railsback, L.B., Bouker, P.A., Feeney, T.P., Goddard, E.A., Hall, A.S., Jackson, B.P., McClain, A.A., Orsega, M.C., Rafter, M.A., Webster, J.W., 1996. A survey of the major-element geochemistry of Georgia groundwater. *Southeastern Geol.* **36** (3), 99–122.

Redfield, A.C., 1934. On the proportions of organic derivatives in sea water and their relation to the composition of Plankton. In: Daniel, R.J. (Ed.), *James Johnstone Memorial Volume*. Liverpool University Press, Liverpool, pp. 177–192.

Redfield, A.C., 1958. The biological control of chemical factors in the environment. *Am. Sci.* **46**, 205–221.

Schulten, H.-R., Schnitzer, M., 1997. The chemistry of soil organic nitrogen: a review. *Biol. Fertil. Soils* **26** (1), 1–15.

Showstack, R., 2000. Nutrient over-enrichment implicated in multiple problems in U.S. waterways. *EOS* **81** (43), 497–499.

Smith, R., Bohlke, J., Garabedian, S., Revesz, K., Yoshinari, T., 2004. Assessing denitrification in groundwater using natural gradient tracer tests with ^{15}N: in situ measurement of a sequential multistep reaction. *Water Resour. Res.* **40**, 1–17.

Straub, K.L., Benz, M., Schink, B., Widdel, F., 1996. Anaerobic, nitrate-dependent microbial oxidation of ferrous iron. *Appl. Environ. Microbiol.* **62** (4), 1458–1460.

Stumm, W., Morgan, J.J., 1996. *Chemical Equilibria and Rates in Natural Waters*. Wiley, New York.

Tesoriero, A., Liebscher, H., Cox, S., 2000. Mechanism and rate of denitrification in an agricultural watershed: electron and mass balance along groundwater flow paths. *Water Resour. Res.* **36** (6), 1545–1559.

Thauer, R.K., Jungermann, K., Decker, K., 1977. Energy conservation in chemotrophic anaerobic bacteria. *Bacteriol. Rev.* **41**, 100–180.

Ueda, S., Go, C., Suzumura, M., Sumi, E., 2003. Denitrification in a seashore sandy deposit influenced by groundwater discharge. *Biogeochemistry* **63** (2), 187–205.

Ueda, S., Ogura, N., Wada, E., 1991. Nitrogen stable isotope ratio of groundwater N_2O. *Geophys. Res. Lett.* **18** (8), 1449–1452.

UNEP. 2003. GEO Year Book 2003. United Nations Environment Programme.

Vairavamurthy, A., Wang, S., 2002. Organic nitrogen in geomacromolecules: insights on speciation and transformation with K-Edge XANES spectroscopy. *Environ. Sci. Technol.* **36**, 3050–3056.

van Groenigen, J., Kuikman, P., de Groot, W., Velthof, G., 2005. Nitrous oxide emission from urine-treated soil as influenced by urine composition and soil physical conditions. *Soil Biol. Biochem.* **37**, 463–473.

Washington, J.W., Cameron, B.A., 2001. Evaluating degradation rates of chlorinated organics in groundwater using analytical models. *Environ. Toxicol. Chem.* **20**, 1909–1915.

Washington, J.W., Endale, D.M., Samarkina, L.P., Chappell, K.E., 2004. Kinetic control of oxidation state at thermodynamically buffered potentials in subsurface waters. *Geochim. Cosmochim. Acta* **68** (23), 4831–4842.

Wilhelm, E., Battino, R., Wilcock, R.J., 1977. Low-pressure solubility of gases in liquid water. *Chem. Rev.* **77**, 219–262.

Willett, V.B., Reynolds, B.A., Stevens, P.A., Ormerod, S.J., Jones, D.L., 2004. Dissolved organic nitrogen regulation in freshwaters. *J. Environ. Qual.* **33**, 201–209.

Winter, T.C., Harvey, J.W., Franke, O.L., Alley, W.M., 1998. *Ground Water and Surface Water: A Single Resource*. United States Geological Survey, pp. 79.

Zang, X., van Heemst, J.D.H., Dria, K.J., Hatcher, P.G., 2000. Encapsulation of protein in humic acid from a histosol as an explanation for the occurrence of organic nitrogen in soil and sediment. *Org. Geochem.* **31**, 679–695.

Zubay, G., 1993. *Biochemistry*. Wm. C. Brown Publishers.